High-precision x-ray FEL pulse arrival time measurements at SACLA by a THz streak camera with Xe clusters

P. N. Juranić,[1,*] A. Stepanov,[1] R. Ischebeck,[1] V. Schlott,[1] C. Pradervand,[1] L. Patthey,[1] M. Radović,[1] I. Gorgisyan,[1,2] L. Rivkin,[1,2] C. P. Hauri,[1,2] B. Monoszlai,[1,3] R. Ivanov,[4] P. Peier,[4] J. Liu,[5] T. Togashi,[6] S. Owada,[7] K. Ogawa,[7] T. Katayama,[7] M. Yabashi,[7] and R. Abela[1]

[1]*Paul Scherrer Institut, 5232 Villigen, Switzerland*
[2]*Ecole Polytechnique Federale de Lausanne, 1015 Lausanne, Switzerland*
[3]*University of Pécs, 7624 Hungary*
[4]*Deutsches Elektronen-Synchrotron, 22607 Hamburg, Germany*
[5]*European XFEL GmbH, 22761 Hamburg, Germany*
[6]*Japan Synchrotron Radiation Research Institute, Sayo, Hyogo 6795198, Japan*
[7]*RIKEN SPring—8 Center, Sayo, Hyogo 6795148, Japan*
**pavle.juranic@psi.ch*

Abstract: The accurate measurement of the arrival time of a hard X-ray free electron laser (FEL) pulse with respect to a laser is of utmost importance for pump-probe experiments proposed or carried out at FEL facilities around the world. This manuscript presents the latest device to meet this challenge, a THz streak camera using Xe gas clusters, capable of pulse arrival time measurements with an estimated accuracy of several femtoseconds. An experiment performed at SACLA demonstrates the performance of the device at photon energies between 5 and 10 keV with variable photon beam parameters.

© 2014 Optical Society of America

OCIS codes: (120.0120) Instrumentation, measurement, and metrology; (020.0020) Atomic and molecular physics; (140.2600) Free-electron lasers (FELs).

References and links:

1. W. Ackermann, G. Asova, V. Ayvazyan, A. Azima, N. Baboi, J. Bahr, V. Balandin, B. Beutner, A. Brandt, A. Bolzmann, R. Brinkmann, O. I. Brovko, M. Castellano, P. Castro, L. Catani, E. Chiadroni, S. Choroba, A. Cianchi, J. T. Costello, D. Cubaynes, J. Dardis, W. Decking, H. Delsim-Hashemi, A. Delserieys, G. Di Pirro, M. Dohlus, S. Dusterer, A. Eckhardt, H. T. Edwards, B. Faatz, J. Feldhaus, K. Flottmann, J. Frisch, L. Frohlich, T. Garvey, U. Gensch, C. Gerth, M. Gorler, N. Golubeva, H. J. Grabosch, M. Grecki, O. Grimm, K. Hacker, U. Hahn, J. H. Han, K. Honkavaara, T. Hott, M. Huning, Y. Ivanisenko, E. Jaeschke, W. Jalmuzna, T. Jezynski, R. Kammering, V. Katalev, K. Kavanagh, E. T. Kennedy, S. Khodyachykh, K. Klose, V. Kocharyan, M. Korfer, M. Kollewe, W. Koprek, S. Korepanov, D. Kostin, M. Krassilnikov, G. Kube, M. Kuhlmann, C. L. S. Lewis, L. Lilje, T. Limberg, D. Lipka, F. Lohl, H. Luna, M. Luong, M. Martins, M. Meyer, P. Michelato, V. Miltchev, W. D. Moller, L. Monaco, W. F. O. Muller, A. Napieralski, O. Napoly, P. Nicolosi, D. Nolle, T. Nunez, A. Oppelt, C. Pagani, R. Paparella, N. Pchalek, J. Pedregosa-Gutierrez, B. Petersen, B. Petrosyan, G. Petrosyan, L. Petrosyan, J. Pfluger, E. Plonjes, L. Poletto, K. Pozniak, E. Prat, D. Proch, P. Pucyk, P. Radcliffe, H. Redlin, K. Rehlich, M. Richter, M. Roehrs, J. Roensch, R. Romaniuk, M. Ross, J. Rossbach, V. Rybnikov, M. Sachwitz, E. L. Saldin, W. Sandner, H. Schlarb, B. Schmidt, M. Schmitz, P. Schmuser, J. R. Schneider, E. A. Schneidmiller, S. Schnepp, S. Schreiber, M. Seidel, D. Sertore, A. V. Shabunov, C. Simon, S. Simrock, E. Sombrowski, A. A. Sorokin, P. Spanknebel, R. Spesyvtsev, L. Staykov, B. Steffen, F. Stephan, F. Stulle, H. Thom, K. Tiedtke, M. Tischer, S. Toleikis, R. Treusch, D. Trines, I. Tsakov, E. Vogel, T. Weiland, H. Weise, M. Wellhoffer, M. Wendt, I. Will, A. Winter, K. Wittenburg, W. Wurth, P. Yeates, M. V. Yurkov, I. Zagorodnov, and K. Zapfe, "Operation of a free-electron laser from the extreme ultraviolet to the water window," Nat. Photonics **1**(6), 336–342 (2007).
2. P. Emma, R. Akre, J. Arthur, R. Bionta, C. Bostedt, J. Bozek, A. Brachmann, P. Bucksbaum, R. Coffee, F. J. Decker, Y. Ding, D. Dowell, S. Edstrom, A. Fisher, J. Frisch, S. Gilevich, J. Hastings, G. Hays, P. Hering, Z. Huang, R. Iverson, H. Loos, M. Messerschmidt, A. Miahnahri, S. Moeller, H. D. Nuhn, G. Pile, D. Ratner, J. Rzepiela, D. Schultz, T. Smith, P. Stefan, H. Tompkins, J. Turner, J. Welch, W. White, J. Wu, G. Yocky, and J.

Galayda, “First lasing and operation of an angstrom-wavelength free-electron laser,” Nat. Photonics **4**(9), 641–647 (2010).
3. T. Ishikawa, H. Aoyagi, T. Asaka, Y. Asano, N. Azumi, T. Bizen, H. Ego, K. Fukami, T. Fukui, Y. Furukawa, S. Goto, H. Hanaki, T. Hara, T. Hasegawa, T. Hatsui, A. Higashiya, T. Hirono, N. Hosoda, M. Ishii, T. Inagaki, Y. Inubushi, T. Itoga, Y. Joti, M. Kago, T. Kameshima, H. Kimura, Y. Kirihara, A. Kiyomichi, T. Kobayashi, C. Kondo, T. Kudo, H. Maesaka, X. M. Marechal, T. Masuda, S. Matsubara, T. Matsumoto, T. Matsushita, S. Matsui, M. Nagasono, N. Nariyama, H. Ohashi, T. Ohata, T. Ohshima, S. Ono, Y. Otake, C. Saji, T. Sakurai, T. Sato, K. Sawada, T. Seike, K. Shirasawa, T. Sugimoto, S. Suzuki, S. Takahashi, H. Takebe, K. Takeshita, K. Tamasaku, H. Tanaka, R. Tanaka, T. Tanaka, T. Togashi, K. Togawa, A. Tokuhisa, H. Tomizawa, K. Tono, S. K. Wu, M. Yabashi, M. Yamaga, A. Yamashita, K. Yanagida, C. Zhang, T. Shintake, H. Kitamura, and N. Kumagai, “A compact X-ray free-electron laser emitting in the sub-angstrom region,” Nat. Photonics **6**(8), 540–544 (2012).
4. E. Allaria, C. Callegari, D. Cocco, W. M. Fawley, M. Kiskinova, C. Masciovecchio, and F. Parmigiani, “The FERMI@Elettra free-electron-laser source for coherent x-ray physics: photon properties, beam transport system and applications,” New J. Phys. **12**(7), 075002 (2010).
5. P. Oberta, U. Flechsig, and R. Abela, “The SwissFEL facility and its preliminary optics beamline layout,” Proc. SPIE **8078**, 807805 (2011).
6. M. R. Bionta, H. T. Lemke, J. P. Cryan, J. M. Glownia, C. Bostedt, M. Cammarata, J. C. Castagna, Y. Ding, D. M. Fritz, A. R. Fry, J. Krzywinski, M. Messerschmidt, S. Schorb, M. L. Swiggers, and R. N. Coffee, “Spectral encoding of x-ray/optical relative delay,” Opt. Express **19**(22), 21855–21865 (2011).
7. M. Beye, O. Krupin, G. Hays, A. H. Reid, D. Rupp, S. de Jong, S. Lee, W. S. Lee, Y. D. Chuang, R. Coffee, J. P. Cryan, J. M. Glownia, A. Fohlisch, M. R. Holmes, A. R. Fry, W. E. White, C. Bostedt, A. O. Scherz, H. A. Durr, and W. F. Schlotter, “X-ray pulse preserving single-shot optical cross-correlation method for improved experimental temporal resolution,” Appl. Phys. Lett. **100**(12), 121108 (2012).
8. O. Krupin, M. Trigo, W. F. Schlotter, M. Beye, F. Sorgenfrei, J. J. Turner, D. A. Reis, N. Gerken, S. Lee, W. S. Lee, G. Hays, Y. Acremann, B. Abbey, R. Coffee, M. Messerschmidt, S. P. Hau-Riege, G. Lapertot, J. Lüning, P. Heimann, R. Soufli, M. Fernández-Perea, M. Rowen, M. Holmes, S. L. Molodtsov, A. Föhlisch, and W. Wurth, “Temporal cross-correlation of x-ray free electron and optical lasers using soft x-ray pulse induced transient reflectivity,” Opt. Express **20**(10), 11396–11406 (2012).
9. M. Harmand, R. Coffee, M. R. Bionta, M. Chollet, D. French, D. Zhu, D. M. Fritz, H. T. Lemke, N. Medvedev, B. Ziaja, S. Toleikis, and M. Cammarata, “Achieving few-femtosecond time-sorting at hard X-ray free-electron lasers,” Nat. Photonics **7**(3), 215–218 (2013).
10. I. Grguraš, A. R. Maier, C. Behrens, T. Mazza, T. J. Kelly, P. Radcliffe, S. Dusterer, A. K. Kazansky, N. M. Kabachnik, T. Tschentscher, J. T. Costello, M. Meyer, M. C. Hoffmann, H. Schlarb, and A. L. Cavalieri, “Ultrafast X-ray pulse characterization at free-electron lasers,” Nat. Photonics **6**(12), 852–856 (2012).
11. U. Frühling, M. Wieland, M. Gensch, T. Gebert, B. Schutte, M. Krikunova, R. Kalms, F. Budzyn, O. Grimm, J. Rossbach, E. Plonjes, and M. Drescher, “Single-shot terahertz-field-driven x-ray streak camera,” Nat. Photonics **3**(9), 523–528 (2009).
12. F. Tavella, N. Stojanovic, G. Geloni, and M. Gensch, “Few-femtosecond timing at fourth-generation x-ray light sources,” Nat. Photonics **5**(3), 162–165 (2011).
13. S. Düsterer, P. Radcliffe, C. Bostedt, J. Bozek, A. L. Cavalieri, R. Coffee, J. T. Costello, D. Cubaynes, L. F. DiMauro, Y. Ding, G. Doumy, F. Gruner, W. Helml, W. Schweinberger, R. Kienberger, A. R. Maier, M. Messerschmidt, V. Richardson, C. Roedig, T. Tschentscher, and M. Meyer, “Femtosecond x-ray pulse length characterization at the Linac Coherent Light Source free-electron laser,” New J. Phys. **13**(9), 093024 (2011).
14. R. Riedel, A. Al-Shemmary, M. Gensch, T. Golz, M. Harmand, N. Medvedev, M. J. Prandolini, K. Sokolowski-Tinten, S. Toleikis, U. Wegner, B. Ziaja, N. Stojanovic, and F. Tavella, “Single-shot pulse duration monitor for extreme ultraviolet and X-ray free-electron lasers,” Nat Commun **4**, 1731 (2013).
15. P. N. Juranić, A. Stepanov, P. Peier, C. P. Hauri, R. Ischebeck, V. Schlott, M. Radovic, C. Erny, F. Ardana-Lamas, B. Monoszlai, I. Gorgisyan, L. Patthey, and R. Abela, “A scheme for a shot-to-shot, femtosecond-resolved pulse length and arrival time measurement of free electron laser x-ray pulses that overcomes the time jitter problem between the FEL and the laser,” J. Instrum. **9**(03), P03006 (2014).
16. M. Hentschel, R. Kienberger, C. Spielmann, G. A. Reider, N. Milosevic, T. Brabec, P. Corkum, U. Heinzmann, M. Drescher, and F. Krausz, “Attosecond metrology,” Nature **414**(6863), 509–513 (2001).
17. M. Drescher, M. Hentschel, R. Kienberger, G. Tempea, C. Spielmann, G. A. Reider, P. B. Corkum, and F. Krausz, “X-ray pulses approaching the attosecond frontier,” Science **291**(5510), 1923–1927 (2001).
18. M. Uiberacker, E. Goulielmakis, R. Kienberger, A. Baltuska, T. Westerwalbesloh, U. Keineberg, U. Heinzmann, M. Drescher, and F. Krausz, “Attosecond metrology with controlled light waveforms,” Laser Phys. **15**, 195–204 (2005).
19. B. L. Henke, E. M. Gullikson, and J. C. Davis, “X-ray interactions-photoabsorption, scattering, transmission, and reflection at E=50-30,000 eV, z=1-92,” At. Data Nucl. Data Tables **54**(2), 181–342 (1993).
20. D. Irimia, D. Dobrikov, R. Kortekaas, H. Voet, D. A. van den Ende, W. A. Groen, and M. H. M. Janssen, “A short pulse (7 micros FWHM) and high repetition rate (dc-5 kHz) cantilever piezovalve for pulsed atomic and molecular beams,” Rev. Sci. Instrum. **80**(11), 113303 (2009).
21. O. F. Hagena and W. Obert, “Cluster formation in expanding supersonic jets-effect of pressure, temperature, nozzle size, and test gas,” J. Chem. Phys. **56**(5), 1793 (1972).

#222011 - $15.00 USD Received 1 Sep 2014; revised 4 Nov 2014; accepted 9 Nov 2014; published 24 Nov 2014
(C) 2014 OSA

22. R. Karnbach, M. Joppien, J. Stapelfeldt, J. Wormer, and T. Moller, "Clulu - an experimental setup for luminescence measurements on Van-Der-Waals clusters with synchrotron-radiation," Rev. Sci. Instrum. **64**(10), 2838–2849 (1993).
23. K. Tono, T. Togashi, Y. Inubushi, T. Sato, T. Katayama, K. Ogawa, H. Ohashi, H. Kimura, S. Takahashi, K. Takeshita, H. Tomizawa, S. Goto, T. Ishikawa, and M. Yabashi, "Beamline, experimental stations and photon beam diagnostics for the hard x-ray free electron laser of SACLA," New J. Phys. **15**(8), 083035 (2013).
24. J. Hebling, G. Almasi, I. Z. Kozma, and J. Kuhl, "Velocity matching by pulse front tilting for large area THz-pulse generation," Opt. Express **10**(21), 1161–1166 (2002).
25. A. G. Stepanov, S. Henin, Y. Petit, L. Bonacina, J. Kasparian, and J. P. Wolf, "Mobile source of high-energy single-cycle terahertz pulses," Appl. Phys. B **101**(1-2), 11–14 (2010).
26. A. G. Stepanov, S. Henin, Y. Petit, L. Bonacina, J. Kasparian, and J. P. Wolf, "Mobile source of high-energy single-cycle terahertz pulses (vol 101, pg 11, 2010)," Appl. Phys. B **115**, 293 (2014).
27. A. B. Ruffin, J. V. Rudd, J. F. Whitaker, S. Feng, and H. G. Winful, "Direct observation of the Gouy phase shift with single-cycle terahertz pulses," Phys. Rev. Lett. **83**(17), 3410–3413 (1999).
28. T. Sato, T. Togashi, K. Ogawa, T. Katayama, Y. Inubushi, K. Tono, and M. Yabashil, "Highly efficient arrival timing diagnostics for femtosecond X-ray and optical laser pulses," Appl. Phys. Express. in press).

1. Introduction

Laser pump, X-ray probe experiments performed at FEL facilities around the world [1–5] typically make use of short pulse length and intense coherent X-ray radiation to perform experiments with sub-picosecond time resolution. As they advance towards improved temporal resolutions, the experiments require accurate measurements of the arrival times of the FEL pulses relative to a laser pump on the sample they are probing. This measurement must also be non-invasive, allowing the maximum use of the X-ray beam for the experiment rather than for diagnostics.

Several methods have been proposed and implemented in the past to meet this diagnostics challenge: transmission/reflectivity spatial and spectral encoding used for soft and hard X-rays at FLASH, SACLA, and LCLS [6–9], the THz streak camera for soft X-rays at FLASH [10,11] as well as other methods [12–14]. All these methods have some advantages but also drawbacks. Some require extensive infrastructure and dedicated beamlines [12,14]. Others are not single-shot measurements [13], or are not completely transparent [6–9], causing degradation of the FEL X-ray beam. The only method that has been attempted for hard x-ray arrival time measurement is the spatial/spectral encoding setup, which has an arrival time accuracy of on the order of 10 fs RMS [6,9]. The potentially more accurate THz streak camera has not been attempted for use at hard X-ray sources due to the small photoionization cross-section of the gas target and the difficulties in differentiating jitters in the photon energy of the FEL beam from an arrival time signal of the FEL beam by electron spectroscopy. The Photon Arrival and Length Monitor (PALM) prototype chamber [15] developed at the Paul Scherrer Institut (PSI) for the future SwissFEL facility mitigates both of these problems, measuring the arrival times of hard X-ray FEL pulses relative to a THz pulse (and the laser it is generated from) with an estimated accuracy of about 4 fs RMS at 9 keV. The presented results obtained at SACLA represent the first measurement of its kind.

2. Concepts

The concept of the THz streak camera has been explained in the past in literature [16–18], and has is capable of measuring pulse lengths of high-harmonic-generation (HHG) soft X-rays at table-top laser laboratories. The device can also be used to measure the arrival time of the X-ray relative to the THz pulse.

The THz streak camera uses a gas that is photoionized by the X-ray light as an electron emitter. The electrons are then subject to a time-varying vector potential generated by co-propagating THz radiation, the duration of which is longer than the pulse length of the X-ray pulse. A shift in the arrival time of the X-ray pulse translates to a shift in the kinetic energy gained by the electrons in the vector potential. The final kinetic energy of the photoelectrons K_f streaked by the vector potential U_p is

#222011 - $15.00 USD Received 1 Sep 2014; revised 4 Nov 2014; accepted 9 Nov 2014; published 24 Nov 2014
(C) 2014 OSA

$$K_f = K_0 + 2U_p \sin^2(\varphi_0) \pm \sqrt{8K_0U_p}\sin(\varphi_0) \quad (1)$$

where K_0 is the initial kinetic energy of the electrons at the time of ionization, φ_0 is the phase of the vector potential at the time of the ionization, the ± depends on the orientation of the THz field, and

$$U_p = \frac{e^2 E_{THz}^2(t)}{4m_e\omega_{THz}^2} \quad (2)$$

$E_{THz}(t)$ is the THz electric field, e is the electron charge, m_e is the mass of the electron, and ω_{THz} is the angular frequency of the THz field.

The time delay between the external THz field and the FEL pulse was controlled mechanically by a LTM60 translation stage, and time of flight of the electrons under different time delays were recorded, forming a two dimensional (2D) streaked spectrogram. As shown in Eq. (1), the shape of the spectrogram is determined by the THz frequency, the initial electron kinetic energy and the vector potential. The time-to-energy map is extracted by recording the center of mass (COM) kinetic energy of each time delay over several hundred shots. The shot-to-shot arrival times of the FEL pulses related to the THz pulse are retrieved by recording the single-shot electron kinetic energy when the delay stage was set at the middle of the time-to-energy slope. The area of interest, between 2 and 3.5 ps in Fig. 2, is sinusoidal, justifying the use of Eq. (1).

Since X-ray photoionization cross sections decrease as the X-ray photon energy increases [19], fewer electrons are thus expected to be generated from single-shot ionization of the noble gas atoms by hard X-rays. However, the PALM setup counterbalances this effect by using Xe gas clusters generated by a supersonic pulsed valve [20] that is synchronized to the FEL pulse, increasing the sample density in the interaction region, while also decreasing the gas load in the streaking chamber. The setup for Xe had a Hagena parameter [21] of about 6800, for which we expected clusters of several hundred to a thousand atoms [22]. The clusters are injected into the interaction region only when the X-ray pulses are passing through, guaranteeing that sufficient electrons are generated for measurement and good statistics. We estimate that between 50 and 500 electrons were in the peaks used for analysis for the monochromator, comparable to the data shown in [11], and about an order of magnitude more without the monochromator.

3. Experimental setup

The experimental chamber, built out of μ-metal and described in [15], was installed at the BL3 beamline at the SACLA FEL facility [3,23]. As shown in Fig. 1, two ETF20 Kaesdorf electron time-of-flight (eTOF) spectrometers measured the strength of the streak induced on the photoelectrons by the vector potential of the THz field. This tandem measurement is used to eliminate the photon energy jitter common at FELs from the observed spectra.

#222011 - $15.00 USD Received 1 Sep 2014; revised 4 Nov 2014; accepted 9 Nov 2014; published 24 Nov 2014
(C) 2014 OSA

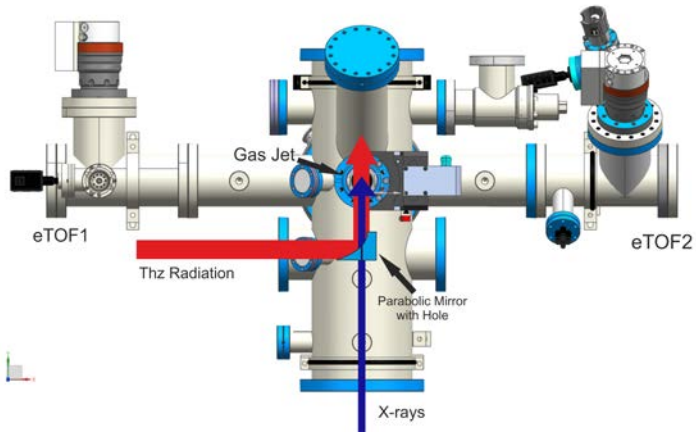

Fig. 1. Schematic drawing of the PALM prototype chamber.

The two e-TOF spectrometers, positioned opposite each other, measure exact opposite streaking effects, but observe the same electron kinetic energy shift due to photon energy jitter. The resolution of the eTOFs over the dynamic range of the measurement is controlled by adjusting their drift tube and electrostatic lens settings. By subtracting the average of the two mean kinetic energies from each individual measurement, the photon energy jitter contribution is eliminated, leaving only the clean measurement of the FEL relative pulse arrival time.

The Xe clusters were injected into the interaction region by a LaserLab Amsterdam piezo cantilever valve [20] synchronously with the 30 Hz SACLA repetition rate. The valve had a 40° conical nozzle with a diameter of 150 μm and a backing pressure of about 3.5 bar above atmospheric pressure. The valve was placed 10 to 12 mm away from the center of the interaction region to deliver the largest amount of gas in the smallest volume possible while not interfering with the flight path of either the THz beam or the FEL pulse. The estimated FWHM diameter of the gas target in the interaction region was about 2.5 mm, and the valve opening time was about 30 μs. The average pressure in the chamber while the valve was working was 1.1×10^{-5} mbar, with a background pressure of about 3×10^{-7} mbar.

SACLA has a 30fs, 800 nm, 7 mJ laser system [23] that was used for the experiment. The THz radiation was generated in a $LiNbO_3$ crystal via the tilted pulse-front pumping method [24] optimized for a high-energy pump [25,26] outside of the chamber and then introduced into vacuum through a z-cut quartz window. The laser intensity was monitored on a shot-to-shot basis to compensate for the change in the THz field's power in the data analysis. The THz beam had a maximum electric field of about 50 kV/cm in the interaction region, and an average frequency of 0.52 THz. A three inch parabolic mirror focused the THz radiation 170 mm downstream, 20 mm behind the interaction region to avoid Gouy phase shift [27] effects across the diameter of the gas target. The 100-200 μm RMS diameter unfocused X-ray FEL pulses were transmitted though the 5 mm hole in the middle of the parabolic mirror and co-propagated with the THz field. The SACLA staff estimated that the laser timing jitter was about 150 fs RMS.

4. Results

The FEL pulse arrival time with respect to the THz pulse was measured at photon energies of 5, 6, 7, 8, 9, and 10 keV with pink (non-monochromatized) FEL pulses with a bandwidth between 0.3- 0.5%. The FEL pulse energy was between 150 and 250 μJ during the run. We observed the streaking effect on the Xe $2p_{3/2}$ photoelectron peak for 6-10 keV and Xe $3d_{5/2}$ peak for the 5 keV photon energy. We also measured the streaking effect at 6, 7, 8, and 9 keV

#222011 - $15.00 USD Received 1 Sep 2014; revised 4 Nov 2014; accepted 9 Nov 2014; published 24 Nov 2014
(C) 2014 OSA

with a Si 111 monochromator, which improves the bandwidth of the photon pulses to about 0.01% at the cost of lowering beam intensity by a factor of about 50. The measurement procedure for every FEL beam setup was the same: after a time-to-energy calibration of the eTOFs, we scanned the high-precision THz delay stage to map out the vector potential, correcting for photon energy jitter as described in section 3, and as shown for 10 keV in Fig. 2. Each time-step measured 100 spectra that fitted the appropriate peaks with a Gaussian function to find the COM kinetic energy of the electrons after retardation. An example of these measurements is shown in Fig. 3. An example of a simultaneous streaked single-shot measurement on both eTOFs is shown in Fig. 4. The eTOF settings were changed for every new setup to ensure the best resolution possible over the whole range of the streaking effect.

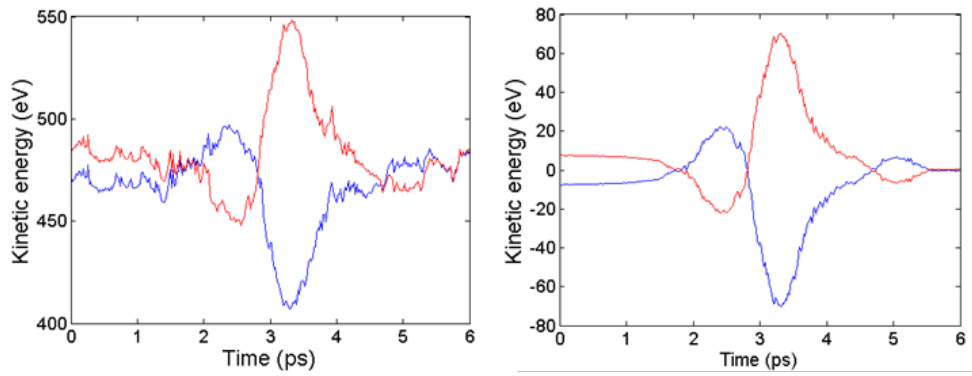

Fig. 2. THz delay scan at 10 keV, raw data (left), and corrected for photon energy jitter and normalized (right). The raw kinetic energies are relative to the retardation and lens settings of the eTOF spectrometers.

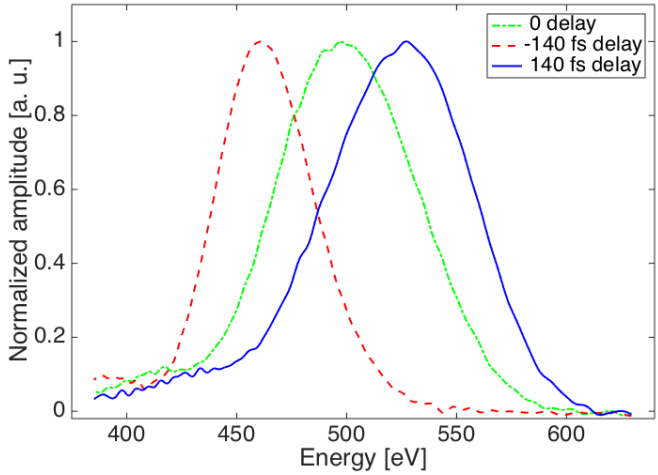

Fig. 3. Average of 100 spectra for FEL delay relative to the middle of the positive THz streak slope for a 10 keV pink beam.

#222011 - $15.00 USD Received 1 Sep 2014; revised 4 Nov 2014; accepted 9 Nov 2014; published 24 Nov 2014
(C) 2014 OSA

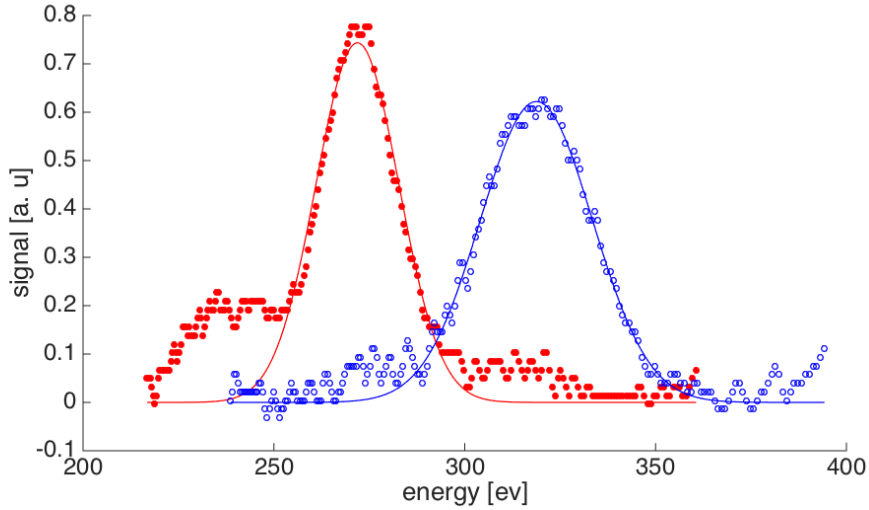

Fig. 4. Example of single-shot streaked spectra taken at 8 keV with the monochromator for the same FEL pulse. The red filled circles are from eTOF1, and the blue hollow circles on the right are from eTOF2, as shown in Fig. 1. The Gaussian fits are representative of the fits we used for our COM estimates.

The THz delay stage was then set in the middle of the leading edge of the streak rise, like the middle of the positive slope of eTOF2 in Fig. 2, to maximize the dynamic range of the arrival time measurements. This gave us a range of about 600 fs in which we could map an arrival time of the FEL beam to a unique kinetic energy of the photoelectron. Figure 5 shows one such arrival time distribution.

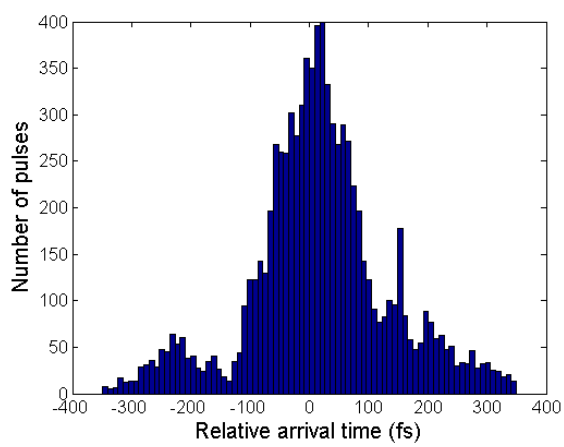

Fig. 5. FEL vs. THz arrival time distribution at 10 keV photon energy with pink beam.

We measured 10,000 spectra from the two eTOFs without the THz beam, with both eTOF spectrometers measuring the same FEL pulse and photoionization processes. We repeated this measurement for every photon energy and eTOF settings to find the RMS accuracy for the mean electron kinetic energy measurements. We estimated the average single-shot arrival time accuracy by taking these measurements, which had COM evaluation accuracies between 0.5 to 1.1 eV RMS, and dividing them by the average slopes of the linear, 300 fs long streaking section of the THz delay scans. The slope values were between 0.11 and 0.32 eV/fs, depending on the photon energy and eTOF settings. The FEL beam began to be unstable at 10

#222011 - $15.00 USD Received 1 Sep 2014; revised 4 Nov 2014; accepted 9 Nov 2014; published 24 Nov 2014
(C) 2014 OSA

keV during the run, preventing monochromator measurements at that photon energy. The monochromator is also not designed to be used at 5 keV, so no monochromator measurements were done at that energy.

The final estimates for accuracy and arrival time jitter values are presented in Table 1. We also took 10,000 spectra at each photon energy and beam mode for our arrival time measurements, of which at least 60%, and typically over 80%, were suitable for a very good Gaussian fit, defined as having a signal-to-noise ratio of 20 and better, and having normalized fit-to-data residuals that were a factor of two or less than the average noise in the spectrum. Note that the accuracy of the measurement decreases linearly with the slope if the arrival time falls out of the linear section of the streak. Conversely, the accuracy of the measurement increases if the arrival time of the FEL falls nearer to the center of the rise slope, in the middle of the linear region. The relative arrival time jitter measurements with the PALM are consistent with previous measurements done at SACLA using their timing tool [28].

Table 1. RMS Arrival Time Jitter between the FEL and Pump Laser Pulses during the Experimental Runs, and Estimated Single-shot Accuracy for the Photon Energies and Modes we Measured with at SACLA

Photon energy, mode	RMS arrival time jitter (fs)	Estimated RMS single-shot accuracy (fs)
5 keV, pink beam	141	6.9
6 keV, pink beam	99	9.5
7 keV, pink beam	121	6.8
8 keV, pink beam	95	5.1
9 keV, pink beam	172	4.0
10 keV, pink beam	119	5.8
6 keV, monochromatic beam	152	4.7
7 keV, monochromatic beam	152	9.5
8 keV, monochromatic beam	91	7.5
9 keV, monochromatic beam	157	8.0

The estimated RMS accuracy numbers in Table 1 make sense when one considers several factors. As Fig. 6 shows, the estimated accuracy of the arrival time measurement goes as the square of the kinetic energy of the ionized electron between 6 and 9 keV with the pink beam, per Eq. (1). However, since the COM fits of a Gaussian profile improve with stronger signal strength in the peak, the 10 keV pink beam accuracy is worse than expected due to the larger pulse energy instability during that part of our experimental run. We used a different electron shell for the 5 keV pink beam measurements, resulting in some inaccuracy due to the difficulties in fitting a Gaussian to the smearing between the Xe $5d_{3/2}$ and Xe $5d_{5/2}$ electrons.

The total signal with the monochromator is significantly reduced compared to the pink beam, resulting in worse estimated arrival time accuracies. The only exception to this rule is the 6 keV monochromatic case, which we believe had a higher signal due to the higher intensity of the SACLA FEL at 6 keV, and a cleaner spectrum after the monochromator when compared to the pink beam at 6 keV. The 6 keV monochromator measurements were also taken at the very end of the SACLA run, while the 6 keV pink beam was measured near the beginning. The additional experience with the experimental and eTOF setup over the course of the beamtime contributed to a better measurement.

#222011 - $15.00 USD Received 1 Sep 2014; revised 4 Nov 2014; accepted 9 Nov 2014; published 24 Nov 2014
(C) 2014 OSA

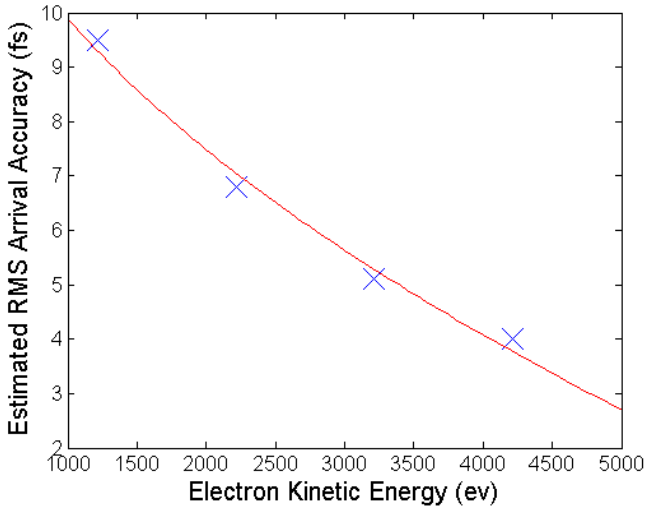

Fig. 6. **:** Electron kinetic energy vs. estimated RMS arrival time accuracy for the pink beam with photon energies between 6 and 9 keV. The blue x's are the kinetic energies, while the solid red line is the square root function fit to the points.

5. Conclusions

The results presented here demonstrate that the PALM device developed at PSI can measure the arrival time of hard X-rays to an accuracy not yet reached by any other method. Since the PALM uses a gas-based measurement method, it is less invasive than most other methods and allows the use of the FEL pulse for experiments further downstream with a minimal loss of intensity or wavefront distortion. The device has shown its effectiveness when working at multiple intensities, being able to measure the arrival time of both the pink and monochromatized FEL beam. It had functioned for the whole 3.5 day beamtime without any problems or interruptions, and with great reliability. In short, the experiment successfully demonstrated that the PALM is a very useful tool for photon diagnostics at hard X-ray FELs.

Acknowledgments

We would like to acknowledge the contribution of the technical staff at PSI and SACLA in the setup and the execution of the experiment, with special thanks to Beat Rippstein, Peter Wiegand, and Goran Marinković. We also thank A. L. Cavalieri for his fruitful discussions with us. We express our acknowledgment to K. Tanaka and H. Hirori for their valuable advice. The experiment was performed with the approval of JASRI (proposal no. 2013B8002).